Original Research

Castrated autoimmune glomerulonephritis mouse model shows attenuated glomerular sclerosis with altered parietal epithelial cell phenotype

Yuki Otani[1], Osamu Ichii[1,2], Md. Abdul Masum[1,3] ⓘ, Takashi Namba[1], Teppei Nakamura[1,4] ⓘ and Yasuhiro Kon[1] ⓘ

[1]Laboratory of Anatomy, Department of Basic Veterinary Sciences, Faculty of Veterinary Medicine, Hokkaido University, Hokkaido 060-0818, Japan; [2]Laboratory of Agrobiomedical Science, Faculty of Agriculture, Hokkaido University, Hokkaido 060-8589, Japan; [3]Department of Anatomy, Histology and Physiology, Faculty of Animal Science and Veterinary Medicine, Sher-e-Bangla Agricultural University, Dhaka 1207, Bangladesh; [4]Department of Biological Safety Research, Chitose Laboratory, Japan Food Research Laboratories, Hokkaido 066-0052, Japan
Corresponding author: Yasuhiro Kon. Email: y-kon@vetmed.hokudai.ac.jp

Impact statement

The prevalence of kidney disease is increasing globally. The loss of kidney function is irreversible, and dialysis and kidney transplantation are the primary treatments; however, they are complex and expensive. Importantly, most patients undergoing dialysis are men. Androgens have been suggested as a risk factor, but how androgens contribute to the pathogenesis of kidney disease remains unclear. Here, we histologically investigated the renal pathology of a glomerulonephritis model and found milder glomerular sclerotic lesions in castrated mice, suggesting an exacerbating effect of androgens on glomerular sclerosis development. Furthermore, we report a clear expression of the androgen receptor in parietal epithelial cells (PECs), but not in glomerular cells, showing altered number and property owing to castration. Taken together, our results provide new evidence that androgens contribute to the pathogenesis of kidney disease by mediating the PEC phenotype; thus, it is crucial to understand the mechanism of male-dominant symptoms.

Abstract

Sex hormones help in maintaining proper immunity as well as renal homeostasis in mammals, and these multi-functional properties characterize the onset of sex-dependent diseases. To clarify the contribution of sex hormones to autoimmune disease-related renal pathogenesis, BXSB/MpJ-*Yaa* was investigated as a murine autoimmune glomerulonephritis model. BXSB/MpJ-*Yaa* and its wild-type, BXSB/MpJ-*Yaa*+ were castrated or sham-operated at three weeks and examined until six months of age. Both castrated strains showed significantly lower serum testosterone levels and body weights than sham-operated mice. Castration did not change the disease phenotypes in BXSB/MpJ-*Yaa*+. At three months, both sham-operated and castrated BXSB/MpJ-*Yaa* manifested splenomegaly, autoantibody production, and glomerulonephritis, and castrated BXSB/MpJ-*Yaa* tended to show heavier spleen weights than the sham-operated group. At six months, both the treated BXSB/MpJ-*Yaa* showed equivalent autoimmune disease conditions; however, castrated mice clearly showed milder glomerular sclerotic lesions than the sham-operated groups. Urinary albumin excretion in castrated BXSB/MpJ-*Yaa* was significantly milder than in sham-operated mice at four months, but those of both the treated BXSB/MpJ-*Yaa* were comparable at six months. The examined renal histopathological indices in parietal epithelial cells were remarkably altered by castration. Briefly, castration decreased the height of parietal epithelial cells and total parietal epithelial cell number in BXSB/MpJ-*Yaa* at six months. For immunostaining, parietal epithelial cells facing the injured glomeruli of BXSB/MpJ-*Yaa* expressed CD44, an activated parietal epithelial cell marker, and CD44-positive parietal epithelial cells showed nuclear localization of the androgen receptor and proliferation marker Ki67. CD44- or Ki67-positive parietal epithelial cells were significantly fewer in castrated group than in sham-operated BXSB/MpJ-*Yaa* at six months. Further, quantitative indices for CD44-positive parietal epithelial cell number and frequency in renal corpuscles positively correlated with glomerular sclerotic severity in BXSB/MpJ-*Yaa*. In conclusion, androgen seemed to have an effect on both systemic immunity and renal morpho-function; however, the effect on the latter could be more clearly observed in BXSB/MpJ-*Yaa*, as parietal epithelial cell activation resulted in glomerular sclerosis.

Keywords: Autoimmune disease, kidney disease, glomerulonephritis, glomerular sclerosis, androgen

Introduction

In mammals, sex hormones play an essential role in maintaining proper reproductive function. In addition, sex hormones have been regarded as modulators of immune function, resulting in clear sex-related disparities in immune system diseases. Systemic lupus erythematosus (SLE), a refractory autoimmune disease showing skin rash, joint pain, and anti-dsDNA autoantibody, represents significant sex-related disparities. SLE incidence rates in pre-menopausal women to age-matched men are 8:1–15:1; however, prevalence is decreased in pre-adolescent and post-menopausal females.[1] These data suggest that estrogens are an exacerbating factor in the etiology of SLE.

Lupus nephritis is the most frequent complication in patients with SLE. Autoimmune factors directly affect the pathogenesis of kidney disease. Besides local inflammation in the kidney due to disrupted autoimmunity, deposition of immune complexes and complement activation lead to thickening of the glomerular basement membrane (GBM), and spike-like structures; in addition, accumulation of extracellular matrix (ECM) produced by mesangial cells and parietal epithelial cells (PECs) results in sclerotic and crescentic lesions in the glomerulus.[2] Importantly, studies have reported that human male patients with SLE show more severe lupus nephritis than women, whereas the prevalence of lupus nephritis in women is higher than that in men due to a higher incidence of SLE.[3,4] This evidence suggests the involvement of sex hormones in the pathogenesis of lupus nephritis, in association with the immune system.

The kidney is an organ that can be affected by sex hormones in terms of development, homeostasis, and disease conditions. Female rats have been reported to have smaller kidneys than males, and castrated mice also have a decreased kidney size.[5] Histologically, the PECs and proximal tubular epithelial cells in mice have been found to be larger in males than in females,[6] suggesting the involvement of androgens in kidney function. Androgen receptor (AR) expression has been confirmed in proximal tubular epithelial cells in mice and rats.[7] In addition, AR mRNA expression was reported in mouse glomeruli, including podocytes, using PCR analysis, and AR proteins in cultured mesangial cells,[7–9] suggesting the contribution of androgens to glomerular homeostasis as well as the pathogenesis of kidney diseases. Clinical studies have reported that several kidney diseases, including glomerulonephritis, glomerulosclerosis, membranous nephropathy, and IgA nephropathy, are more prevalent and serious in males.[10–12] Experimental studies have supported androgens as a risk factor for kidney diseases, as shown by the protective effect of castration in several kidney disease models induced by ureteral obstruction, ischemia-reperfusion, and diabetes;[13–15] in contrast, estrogen is suggested to have a protective role in kidney disease, as demonstrated in human and animal models.[16] On the other hand, for autoimmune nephritis, we have previously reported that androgens play a protective role in pathology of autoimmune glomerulonephritis in congenic mice unlike other kidney disease models.[17] Furthermore, examination

of autoimmune-prone NZB-derived F1 mice showed that estrogen promotes autoimmune glomerulonephritis due to excessive activation of cellular immunity.[18] These results suggest that autoimmune disease-related nephritis is complicatedly formed by systemic autoimmune conditions and sex-related factors.

The BXSB/MpJ-*Yaa* mouse (Yaa) is a representative model of male-dominant systemic autoimmune disease, characterized by autoantibody production and splenomegaly due to the excessive proliferation of autoreactive lymphocytes.[19] Yaa develops severe membranous proliferative glomerulonephritis (MPGN), characterized by glomerular hypertrophy, thickening of GBM, and expansion of sclerotic lesions.[20] Yaa is derived from the BXSB/MpJ-*Yaa*⁺ (BXSB) strain, and is presumed to develop the disease due to Y-linked autoimmune acceleration (*Yaa*) mutations, duplication of some genes on the telomere region of X chromosome to that of the Y chromosome in males.[21] Previous studies revealed that the BXSB genome is also suspected to develop autoimmune disease-prone phenotypes, as aged female BXSB manifested autoantibody production and glomerulonephritis.[22] In addition to *Yaa* mutation, we have reported that podocyte injuries due to the immune-associated genes on chromosome 1 contribute to the etiology of glomerulonephritis in Yaa, resulting in albuminuria. The effect of gonadectomy on Yaa was previously reported; there was little effect on their phenotypes; nevertheless, castrated Yaa was slightly accelerated to develop the autoimmune disease.[23] However, detailed pathology of autoimmune glomerulonephritis in Yaa, contributed by sex hormones has not been discussed so far.

In the present study, we histologically investigated the influence of castration on the pathogenesis of systemic autoimmune disease and glomerulonephritis in Yaa. Castrated Yaa accelerated the development of the autoimmune disorder represented by early splenomegaly at three months, but there was no difference in renal pathology. At six months, castrated Yaa clearly showed milder sclerotic lesions in glomeruli, although autoimmune indices were equivalent between treatments. These results show that androgens mediate the onset of systemic autoimmune disease condition at an early stage but exacerbate glomerular sclerosis with priority over the effect of autoimmunity in the later stages of the disease in Yaa.

Materials and methods

Animals and sample preparation

BXSB (without *Yaa* mutation) and Yaa mice were purchased from Japan SLC, Inc. (Hamamatsu, Shizuoka, Japan). Mice were castrated or sham-operated at three-weeks-old, under combination anesthesia (0.3 mg/kg of medetomidine, 4.0 mg/kg of midazolam, and 5.0 mg/kg of butorphanol) with buprenorphine (0.1 mg/kg). First, the middle of the scrotum was incised in both the treated groups. Testes from both sides, epididymis, and part of the deferent duct were removed in the castrated group. During sham-operation, the testes were just held and pulled lightly, and then were placed back into the scrotum. Mice were

maintained according to the Guide for the Care and Use of Laboratory Animals of Hokkaido University, and all animal experiments were approved by the Institutional Animal Care and Use Committee of Hokkaido University and the Faculty of Veterinary Medicine, Hokkaido University (approval No. 15–0079, 20–0012). Our animal experiment program was approved by the Association for Assessment and Accreditation of Laboratory Animal Care International. Urine was continuously collected from mice three to six months of age, by pressure urination. At three- or six-months old, under deep anesthesia, after body weights were measured, blood samples were collected by cutting the carotid artery. After euthanasia by cervical dislocation, the kidney and spleen were collected. The weights of the kidney and spleen were measured, and the ratio to body weight was compared in each group.

Serological and urinary analyses

Serum and urine were used to evaluate physiological parameters. Serum testosterone levels were measured using the Testosterone ELISA Kit (IBL, Gunma, Japan), to evaluate male reproductive functions. In addition, serum anti-double-stranded DNA (dsDNA) antibody levels were measured using the Mouse Anti-dsDNA ELISA Kit (Shibayagi, Gunma, Japan), to evaluate systemic autoimmune conditions. As for renal function analysis, serum blood urea nitrogen (BUN) and serum creatinine (Cre) were measured using a Fuji Dri-Chem 7000v instrument (Fujifilm, Tokyo, Japan). Urinary albumin and creatinine levels were measured using the LBIS Mouse Albumin ELISA Kit (FUJIFILM Wako Pure Chemical Corporation) and Urinary Creatinine Assay Kit (Detroit R&D, Inc.; Detroit, MI, USA), and subsequently, the urinary albumin creatinine ratio (uACR) was calculated. We followed the manufacturer's instructions for performing all the assays.

Histological analysis

The collected organs were fixed in 4% paraformaldehyde for approximately 24 h. After embedding in paraffin, kidney samples were cut into 2-μm thick sections. The sections were deparaffinized and then stained with periodic acid-Schiff-hematoxylin (PAS-H), periodic acid methenamine-silver (PAM), and Masson's trichrome (MT) stains. In histoplanimetrical analysis, histological sections were converted into digital images by scanning with NanoZoomer 2.0-RS (Hamamatsu Photonics K.K., Shizuoka, Japan). Nuclear numbers in the glomerulus and glomerular area were quantified using the NDP.view2 program (Hamamatsu Photonics K.K., Shizuoka, Japan). The sclerotic lesion area of more than 20 glomeruli was measured using sections stained with MT, using a BX analyzer (Keyence, Osaka, Japan), and the sclerotic lesion fraction was calculated as the percentage of the sclerotic area to the glomerular area.

Immunostaining

Deparaffinized sections were treated for antigen retrieval in 20 mM Tris-HCl buffer (pH 9.0) at 110°C for 15 min.

For immunohistochemistry, sections were soaked in methanol containing 0.3% H_2O_2 for 20 min at room temperature. After washing and blocking with normal goat or donkey serum for 1 h at room temperature, sections were incubated with primary antibodies, listed in Table 1, at 4°C for over 16 h. After washing, the sections were incubated with secondary antibodies, listed in Table 1. For immunohistochemistry, the sections were incubated with streptavidin-horseradish peroxidase (SABPO kit; Nichirei, Tokyo, Japan) for 30 min at room temperature, and then incubated with 3,3-diaminobenzidine tetrahydrochloride-0.3% H_2O_2 solution. Finally, the sections were counterstained with hematoxylin. For immunofluorescence, sections were incubated with Hoechst 33342 (1:500; Dojindo, Kumamoto, Japan) for nuclear staining at room temperature for 15 min. All the immunofluorescence sections were observed under an All-in-One Fluorescence Microscope BZ-X710 (Keyence, Osaka, Japan), and were analyzed using a BX analyzer.

In histoplanimetrical analysis, immunostained sections for CD44 were converted into digital images by scanning with NanoZoomer 2.0-RS. With more than 50 renal corpuscles, the total number and CD44-positive PECs were counted, and the circumference length of each Bowman's capsule was measured with the NDP.view2 program. Then, the numbers of total and CD44-positive PECs per unit length of Bowman's capsules were calculated. In addition, the number of renal corpuscles, including the CD44-positive PECs as well as the total number of renal corpuscles in a section was calculated, followed by the evaluation of CD44-positive renal corpuscle ratio. Further, in immunofluorescent sections, the number of antigens identified using monoclonal antibody Ki67 (Mki67, also known as Ki67)-positive PECs was counted by observing under a BZ-X710 microscope, in more than 100 renal corpuscles, and the number of Ki67-positive PECs in a renal corpuscle was calculated.

Reverse transcription and quantitative PCR

Total RNA was isolated from the kidneys using TRIzol Reagent (Life Technologies, Carlsbad, CA, USA), following the manufacturer's protocol. cDNA was synthesized from total RNA by reverse transcription (RT) using the ReverTra Ace qPCR RT Master Mix with gDNA Remover (TOYOBO, Osaka, Japan). Gene expression levels were examined using synthesized cDNA, THUNDERBIRD SYBR qPCR Mix (TOYOBO, Osaka, Japan), and a real-time thermal cycler (CFX Connect; BIO-RAD, California, USA), following the manufacturer's instructions. Gene expression in the kidneys was normalized to the expression of actin beta (*Actb*). The details of the primers are shown in Table 2.

Statistical analysis

The results are expressed as mean ± standard error (SE), and were analyzed using non-parametric statistical methods. Data between different treatments in the same strain, different strains with the same treatment, and different ages in the same strain with the same treatment were compared using the Mann–Whitney *U*-test. Spearman's correlation

Table 1. Antibodies.

Primary antibody	Source	Detection (application)	Dilution	Blocking	Antigen retrieval	Secondary antibody (IHC)	Secondary antibody (IF)
Rabbit anti-nephrin	IBL (Gunma, Japan)	Podocyte slit diaphragm (IF)	1:400	5% NDS	10 mM CB (pH 6.0) 110°C, 15 min	–	Alexa Fluor 488-labeled donkey anti-rabbit IgG antibodies (1:500; Thermo Fisher Scientific)
Rabbit anti-podocin	IBL (Gunma, Japan)	Podocyte slit diaphragm (IF)	1:800	5% NDS	10 mM CB (pH 6.0) 110°C, 15 min	–	Alexa Fluor 488-labeled donkey anti-rabbit IgG antibodies (1:500; Thermo Fisher Scientific)
Mouse anti-synaptopodin	Fitzgerald, (MA, USA)	Podocyte cytoskeleton (IF)	1:100	5% NDS	10 mM CB (pH 6.0) 110°C, 15 min	–	Alexa Fluor 546-labeled donkey anti-rabbit IgG antibodies (1:500; Thermo Fisher Scientific)
Rabbit anti-androgen receptor	Abcam (Cambridge, UK)	Androgen receptor (IHC, IF)	1:500 (IHC) 1:200 (IF)	10% NGS (IHC) 5% NDS (IF)	20 mM Tris-HCl (pH 9.0) 121°C, 10 min	Biotin-conjugated goat anti-rabbit IgG antibody (SABPO(R) Kit, Nichirei)	Alexa Fluor 546-labeled donkey anti-rabbit IgG antibodies (1:500; Thermo Fisher Scientific)
Rat anti-CD44	BD Biosciences (CA, USA)	Activated parietal epithelial cell (IHC, IF)	1:400 (IHC) 1:800 (IF)	10% NGS (IHC) 5% NDS (IF)	20 mM Tris-HCl (pH 9.0) 110°C, 15 min	Goat anti-rat IgG antibody (Santa Cruz, CA, USA)	Alexa Fluor 488-labeled donkey anti-rabbit IgG antibodies (1:500; Thermo Fisher Scientific)
Rabbit anti-Ki67	Abcam (Cambridge, UK)	Proliferating cell (IF)	1:800	5% NDS	20 mM Tris-HCl (pH 9.0) 110°C, 15 min	–	Alexa Fluor 546-labeled donkey anti-rabbit IgG antibodies (1:500; Thermo Fisher Scientific)

CB: citrate buffer; NGS: normal goat serum; NDS: normal donkey serum; IHC: immunohistochemistry; IF: immunofluorescence.

coefficient was used to analyze the correlation between two parameters. All the values were considered statistically significant at $P < 0.05$.

Results

Physiological change in castrated mice

We first compared the physiological parameters of sham-operated and castrated mice to evaluate the effect of castration. Figure 1(a) shows the blood testosterone level of each group. All castrated mice at both ages showed significant decrease in their testosterone levels compared with those of sham-operated mice. Body weights of all castrated mice were also lower than those of sham-operated mice of the same strain at three and six months (Figure 1(b)). Castration did not induce any change in the spleen weight of BXSB mice, but decreased the body weight in castrated mice at both ages (Figure 1(c) and (d)). On the other hand, castrated Yaa at three months showed a tendency of increased spleen weight compared to the sham-operated group ($P = 0.083$, Figure 1(c)), which resulted in a significant difference in spleen weight to body weight ratio (Figure 1(d)). On histological examination of the spleen, Yaa showed expanded white bulb area compared to BXSB, but there was no significant difference between the treatment groups (Supplemental Figure 1(a)). At six months, there was no significant difference in spleen weight, body weight ratio, or histology between castrated and sham-operated Yaa (Figure 1(d), Supplemental Figure 1(b)). Serum anti-dsDNA antibody levels were higher in Yaa than in BXSB of all the examined groups, but no difference was observed between castrated and sham-operated mice of both strains at three and six months (Figure 1(e)). These data suggest that castration evidently did not have any effect on the immune system but might affect the onset of autoimmune disease of Yaa.

Histological changes in the kidney of castrated mice

We next examined the histology of the kidneys in mice to investigate the effect of castration on renal pathogenesis. In BXSB, sham-operated mice did not show glomerular pathology at three and six months, and there were no significant histological changes in the glomerulus due to castration (Figure 2(a)). On the other hand, castrated BXSB showed a flattened morphology of PEC, while the sham-operated BXSB rendered a more cuboidal shape at both the ages. Figure 2(b) shows representative glomerular histology of three-month-old Yaa. Both the treated mice showed MPGN with glomerular hypertrophy and expansion of mesangial lesions, but there were no treatment-related histological changes in the renal corpuscle except for flat PEC, as observed in castrated BXSB (Figure 2(b)). At six months, severe MPGN characterized by glomerular hypertrophy, thickened GBM, and expansion of sclerotic lesions was observed in both treatment groups; however, castrated mice showed milder expansion of sclerotic lesions compared with sham-operated mice (Figure 2(c)). Furthermore, some sham-operated Yaa showed more severe MPGN, characterized by global sclerotic lesions

Table 2. Primers.

Gene name (accession no.)	Official symbol	Primer sequence (5'-3')	Product size (bp)
Actin beta (NM_007393)	*Actb*	F: TGTTACCAACTGGGACGACA R: GGGGTGTTGAAGGTCTCAAA	165
Nephrosis 1, nephrin (NM_019459)	*Nphs1*	F: ACCTGTATGACGAGGTGGAGAG R: TCGTGAAGAGTCTCACACCAG	218
Nephrosis 2, podocin (NM_130456)	*Nphs2*	F: AAGGTTGATCTCCGTCTCCAG R: TTCCATGCGGTAGTAGCAGAC	105
Synaptopodin (NM_177340.2)	*Synpo*	F: CATCGGACCTTCTTCCTGTG R: TCGGAGTCTGTGGGTGAG	90
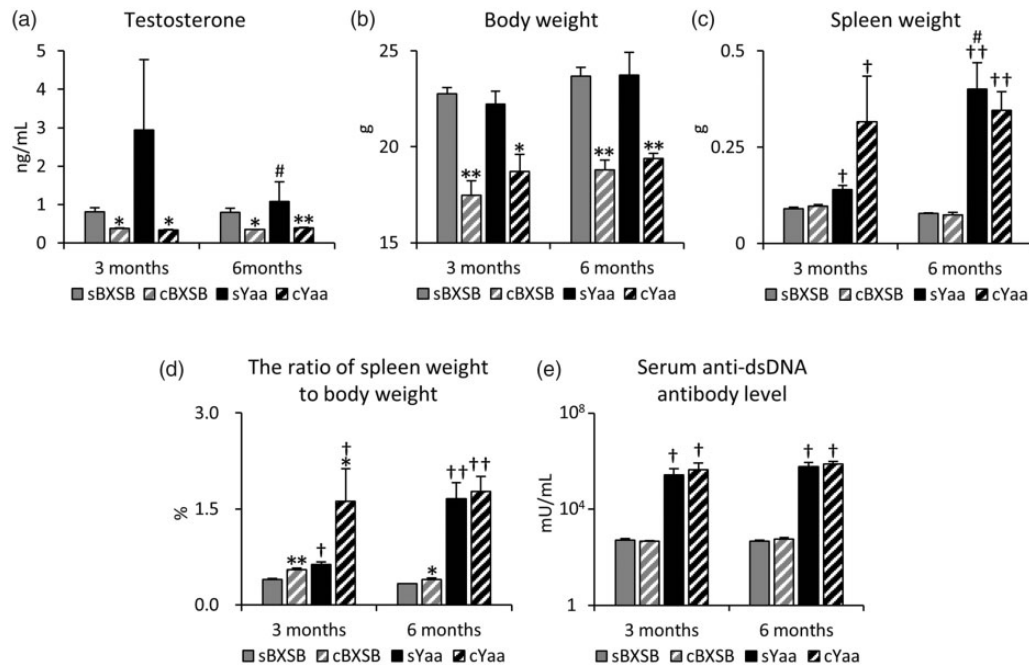
Figure 1. Indices of male reproductive function and autoimmune disease condition in mice. (a) The serum level of testosterone. (b) Body weight. (c) Spleen weight. (d) The ratio of spleen weight to body weight. (e) The serum level of anti-double stranded DNA antibody. Each bar represents mean $\pm$ SE ($n = 4$–10). s: sham-operated; c: castrated. *: Significant differences in castrated groups against sham-operated group in the same strain at the same age (*: $P < 0.05$, **: $P < 0.01$, Mann–Whitney U-test). †: Significant differences in Yaa against BXSB with the same treatment at the same age ($^{\dagger}P < 0.05$, $^{\dagger\dagger}P < 0.01$, Mann–Whitney U-test). #: Significant differences in six-month-old groups against three-month-old groups in the same strain with the same treatment ($^{\#}$: $P < 0.05$, Mann-Whitney U-test).

and crescent formed by stratified PECs and ECM attached to the capillary tuft (Figure 2(d)); however, these pathological changes were scarcely observed in castrated Yaa. Comparison of histoplanimetries between different treatment groups at six months did not alter the area of glomerulus and the number of glomerular nuclei due to castration (Figure 2(e) and (f)). On the other hand, sclerotic lesion area and its fraction of glomerulus were remarkably lower in castrated mice than in sham-operated Yaa (Figure 2(g) and (h)).

Functional changes in podocytes of castrated Yaa kidney

We further investigated the morpho-function of podocytes of six-month-old Yaa, since formation of sclerotic lesions is considered to be the result of loss of podocyte function. Figure 3(a) shows immunofluorescence of podocyte slit diaphragm molecules (nephrin and podocin) and podocyte cytoskeleton molecule (synaptopodin) in Yaa glomerulus at six months. In both the treated Yaa, expression of all the molecules was faint at the center of the glomerulus. On comparing the treatments, partial granular patterns were observed at the glomerular edge in the sham-operated group, but a linear positive reaction was relatively maintained in the castrated Yaa for all the markers. Quantitative PCR analysis showed significantly higher levels of podocyte functional markers in castrated mice than in sham-operated mice (Figure 3(b)).

Loss of podocyte slit diaphragm molecules results in albumin leakage into the urine. Levels of uACR were compared between sham-operated and castrated Yaa from three to six months (Figure 3(c)). At three months, uACR levels were equivalent between the two treatment groups. On the other hand, castrated mice demonstrated significantly decreased levels of uACR at four months compared to sham-operated mice, and this tendency continued till five months, but without statistical significance.
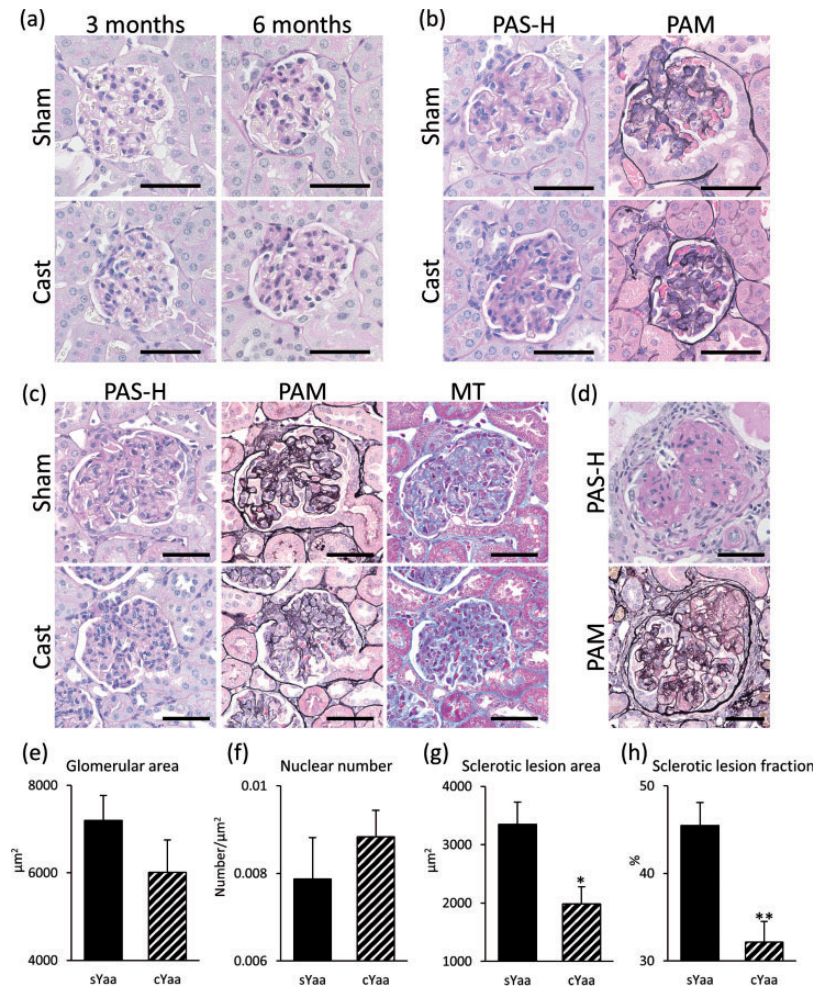
Figure 2. Histopathological analysis of glomeruli in mice. (a) Histology of glomeruli in sham-operated and castrated BXSB at three and six months. Sections are stained with periodic acid-Schiff-hematoxylin (PAS-H). (b and c) Histology of glomeruli in sham-operated and castrated Yaa at three months (b) and six months (c). Sections are stained with PAS-H, periodic acid methenamine-silver (PAM), and Masson's trichrome (MT). At three months, glomerular hypertrophy, increase in mesangial matrix lesion, and wrinkling of the glomerular basement membrane were observed, but there were no treatment-related differences. These histological changes are clearer at six months compared with three months in both the treatment groups. Expansion of sclerotic lesion is more significant in sham-operated Yaa than in castrated Yaa. (d) Representative histology of glomeruli with global sclerotic lesions stained with PAS-H and PAM in sham-operated Yaa at six months. Increased parietal epithelial cells and accumulation of extracellular matrix are significant, resulting in the adhesion of glomerular tuft and Bowman's capsule. Bars = 50 μm. (e) The area of glomeruli in sham-operated Yaa (sYaa) and castrated Yaa (cYaa) at six months. (f) The number of nuclei per unit area of a glomerulus in sYaa and cYaa at six months. (g) The area of sclerotic lesion in glomeruli in sYaa and cYaa at six months. (h) The fraction of sclerotic lesions in sYaa and cYaa at six months. Each bar represents mean ± SE ($n = 8$–10). Significant differences in castrated groups compared to the sham-operated group are indicated with an asterisk. *: $P < 0.05$, **: $P < 0.01$ (Mann–Whitney U-test). (A color version of this figure is available in the online journal.)

Eventually, uACR was comparable between the two groups at six months. Serum BUN and Cre in castrated Yaa were observed to be lower than those in sham-operated mice, but without statistical significance (Figure 3(d) and (e)).

Analysis of androgen receptor in six-month-old Yaa kidney

Next, we examined AR in Yaa kidney to determine the role of androgen in the pathogenesis of glomerulonephritis in Yaa. In six-month-old Yaa, kidney weight was significantly decreased by castration (sham-operated (g): 0.168 ± 0.010, castrated (g): 0.115 ± 0.006). Figure 4(a) shows immunohistochemistry for AR in six-month-old Yaa kidney. In sham-operated kidneys, a clear positive reaction was detected in the nuclei of proximal tubules in the cortex and outer stripe of the outer medulla, and their cytoplasm was slightly

positive. As for the cells in the renal corpuscle, immunopositive reaction was clearly detected in the nuclei of PECs in sham-operated Yaa. Castrated mice showed similar localization of AR in the kidney, but positive reactions in the nuclei of both tubulointerstitium and PECs were relatively weak as compared with those in the sham-operated Yaa. However, on comparing the mRNA levels of *Ar* in Yaa kidney, no difference was observed between sham-operated and castrated mice (Figure 4(b)).

Analysis of PEC phenotype in six-month-old Yaa kidney

PECs have been demonstrated to contribute in the formation of glomerulosclerosis.[24] In particular, activated PECs, characterized by CD44 expression on their cell membrane, are considered to have the potential to migrate, proliferate, and produce ECM, and play a role in the pathogenesis of
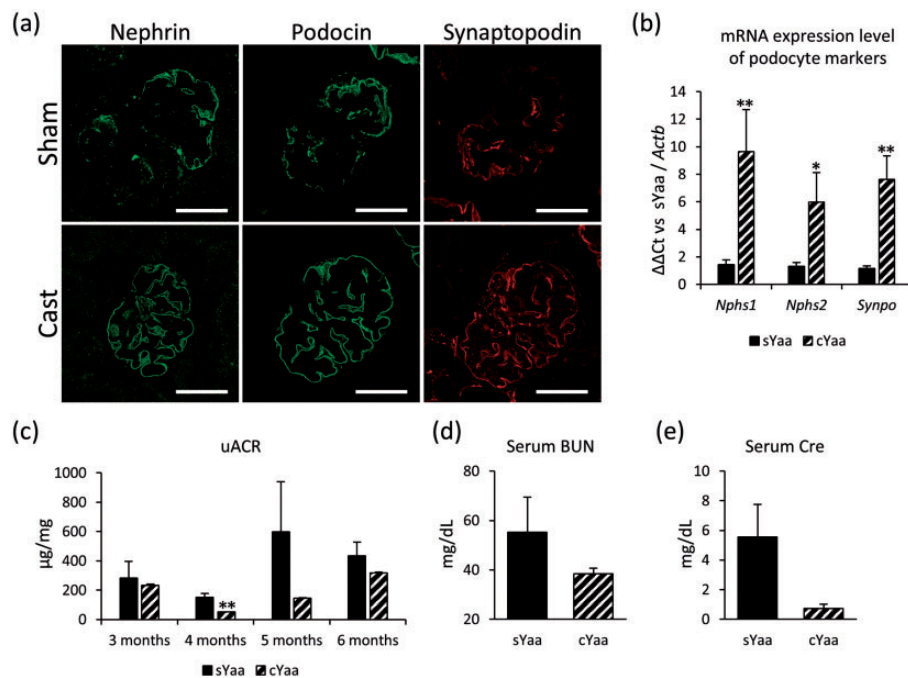
Figure 3. Analysis of podocyte function in six-month-old Yaa. (a) Immunofluorescence of podocyte function molecules (podocin, nephrin, synaptopodin) in Yaa at six months. Nephrin-, podocin- and synaptopodin-immunopositive areas are faint at the center of the glomerulus of Yaa in both the treatment groups, but linear positive reactions at the peripheral area of glomeruli are partially eliminated in only sham-operated groups. Bars = 50 μm. (b) Relative mRNA expression of podocyte function molecules in kidneys of sham-operated Yaa (sYaa) and castrated Yaa (cYaa). The expression levels were normalized to the levels of *Actb*. (c) uACR in sYaa and cYaa from three to six months. (d and e) The serum levels of serum blood urea nitrogen (BUN, d) and serum creatinine (Cre, e) in sYaa and cYaa at six months. Each bar represents mean ± SE ($n = 8$–10). Significant differences in castrated groups compared to the sham-operated group are indicated with an asterisk. *: $P < 0.05$, **: $P < 0.01$ (Mann–Whitney U-test). (A color version of this figure is available in the online journal.)
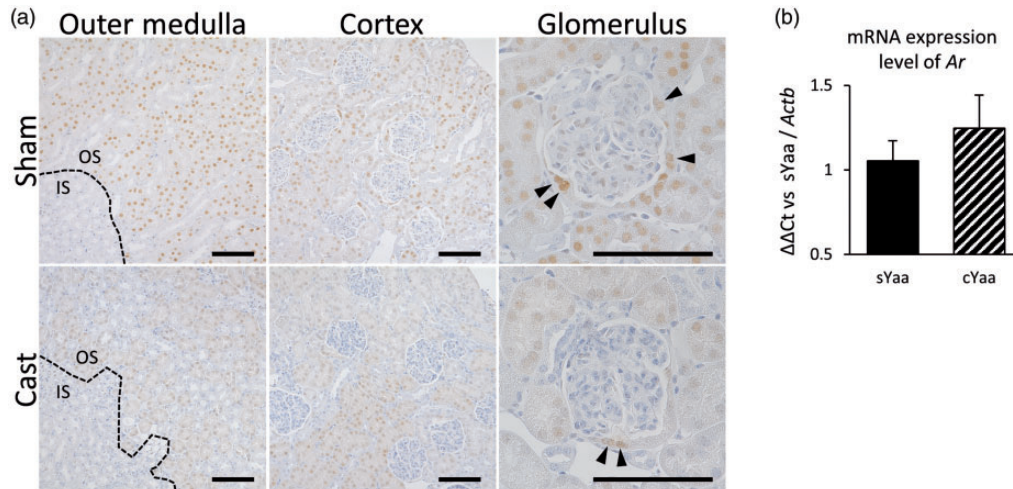

Figure 4. Analysis of androgen receptor in six-month-old Yaa. (a) Immunohistochemistry of androgen receptor (AR) in outer medulla, cortex, and glomerulus of Yaa kidneys at six months. Positive reaction is detected in nucleus of proximal tubules in medulla and cortex, and parietal endothelial cells (PECs). Dotted line represents the boundary between outer stripe (OS) and inner stripe (IS) in outer medulla. Arrowheads represent AR-positive PECs. Both the treatment groups show same localization, but reaction strengths in PECs tend to be lower in castrated Yaa. Bars = 100 μm. (b) Relative mRNA expression of *Ar* in kidneys of sham-operated Yaa (sYaa) and castrated Yaa (cYaa). The expression levels were normalized to the levels of *Actb*. Each bar represents mean ± SE ($n = 8$–10). (A color version of this figure is available in the online journal.)

glomerular sclerotic lesions.[25] We first examined the expression of CD44 in six-month-old Yaa kidneys, using immunohistochemistry. CD44-positive PECs were rarely observed in the renal corpuscle with uninjured glomeruli in both the treated Yaa groups (Figure 5(a)). On the other hand, CD44-positive reaction was clearly observed in the PECs of renal corpuscles with injured glomeruli showing hypertrophy and expansion of sclerotic lesions. Particularly, PECs located in the middle (equatorial) part of Bowman's capsule, representing middle, between flat and cuboidal, height, frequently showed CD44-positive reactions compared to other parts of the PECs in both the groups. These PECs have been classified as intermediate PECs having proliferation and migration properties.[26]
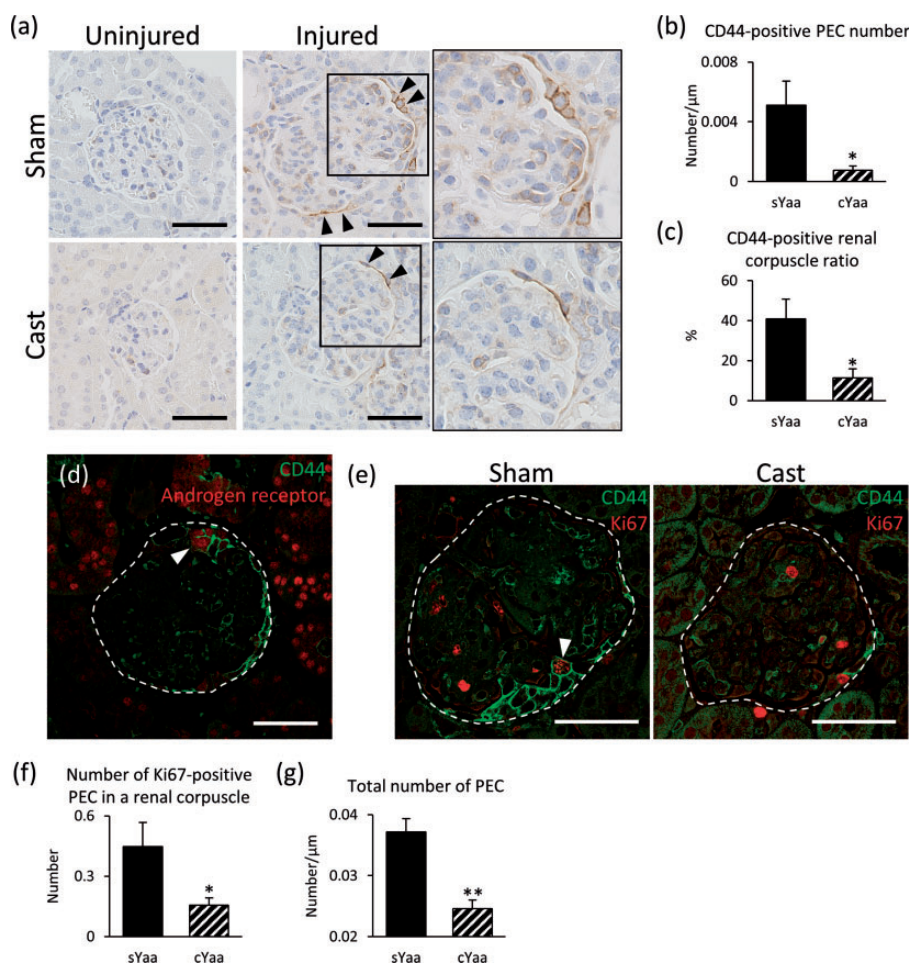
Figure 5. Histopathological analysis of parietal epithelial cells in six-month-old Yaa. (a) Immunohistochemistry of CD44 in Yaa kidneys at six months. Arrowheads represent CD44-positive parietal epithelial cells (PECs). In renal corpuscles with uninjured glomeruli, CD44-positive PECs are not observed in both the treatment groups. PECs in renal corpuscles with injured glomeruli show positive reaction on their cell membrane. Treatment-related change of CD44 localization is not observed. Bars = 50 μm. (b) The number of CD44-positive PECs per unit length of Bowman's capsule in sham-operated Yaa (sYaa) and castrated Yaa (cYaa) at six months. (c) The ratio of renal corpscles with CD44-positive PECs in sYaa and cYaa at six months. (d) Immunofluorescence of androgen receptor (red, AR) and CD44 (green) in sYaa at six months. Dotted line represents renal corpuscles. Arrowheads represent both markers-positive PECs. Some of the CD44-positive PECs stratify, and some of their nuclei are positive for AR. Bar = 50 μm. (e) Immunofluorescence of Ki67 (red) and CD44 (green) in Yaa at six months. Dotted line represents renal corpuscles. Arrowhead represents both markers-positive PECs. Some CD44-positive PECs stratify, and some of their nuclei are positive for Ki67 in sham-operated Yaa. Bars = 50 μm. (f) The number of Ki67-positive PECs in a renal capsule in sYaa and cYaa at six months. (g) The total number of PECs per unit length of Bowman's capsule in sYaa and cYaa at six months. Each bar represents mean ± SE ($n = 8$–10). Significant differences in castrated groups compared to the sham-operated group are indicated with an asterisk. *: $P < 0.05$, **: $P < 0.01$ (Mann–Whitney U-test). (A color version of this figure is available in the online journal.)

Sham-operated Yaa clearly showed CD44 expression on their cell membrane, particularly on the surface facing the capsular lumen, but in castrated mice, cell membrane reaction was unclear due to flat morphology of PECs. In histoplanimetrical analysis, CD44-positive PEC number was significantly decreased in castrated Yaa at six months (Figure 5(b)). Furthermore, castrated mice showed a lower frequency of renal corpuscles with CD44-positive PECs (Figure 5(c)).

Analysis for CD44-related phenotypes in six-month-old Yaa PECs

Figure 5(d) shows immunofluorescence of CD44 and AR in sham-operated Yaa at six months, having glomeruli with sclerotic lesions. Many PECs were positive for CD44, and stratified PECs clearly showed positive reactions for both CD44 and AR. Importantly, AR has been reported to bind to

androgen response elements (ARE), a palindromic and dihexameric motif, in promoters and enhancers of target genes.[27] Chromatin immunoprecipitation sequencing revealed an ideal ARE motif consisting of two hexamers, 5′-AGAACA-3′ and 5′-TGTTCT-3′, with a 3 bp spacer (5′-AGAACANNNTGTTCT-3′).[28] Three half sites of 5′-AGAACA-3′ and one 5′-TGTTCT-3′ were present in a sequence of about 3.0 kb upstream of a *Cd44* gene, whereas no full sequence 5′-AGAACANNNTGTTCT-3′ was present in that region.

For the analysis of proliferating cells, Ki67 was used with immunostaining. Figure 5(e) shows a representative immunofluorescence for CD44 and Ki67 in Yaa kidneys showing MPGN. Ki67-positive cells were observed in the glomerulus and PECs of both the treated Yaa groups at six months. In sham-operated Yaa, in particular, Ki67-positive reactions were observed in the stratified PECs that showed a positive reaction for CD44, whereas stratified

PECs were rarely observed in castrated Yaa. Histoplanimetrical analysis showed a significant decrease in Ki67-positive PEC number in castrated Yaa (Figure 5(f)), and the total number of PECs was also significantly lower in castrated kidneys (Figure 5(g)).

Correlation analysis among examined parameters in six-month-old Yaa

Table 3 shows correlation between sclerotic lesion and examined parameters in six-month-old Yaa of both the treatment groups. The area of sclerotic lesion showed correlation with spleen weight, but sclerotic fraction and uACR showed no correlation with autoimmune disease indices. In addition, CD44 parameters showed weak positive correlation with spleen weight, but not with anti-dsDNA antibody level. Meanwhile, both area and fraction of sclerotic lesions were significantly and positively correlated with PEC parameters, CD44-positive PEC number, CD44-positive renal corpuscle ratio, and total PEC number. The sclerotic area, in particular, showed positive correlation with CD44-positive PEC parameters. Further, uACR was also clearly associated with CD44 expression in PECs, and CD44 parameters showed positive correlation with PEC number.

Discussion

In both healthy and autoimmune disease groups, castration decreased serum testosterone levels and body weight three months onwards. This would be because androgens contribute to increasing the weights of bones and muscles.[29] In the comparison of autoimmune indices, castration seemed to accelerate the onset of autoimmune disease, but did not have any effect on the late pathological stage of Yaa. Splenomegaly is generally observed when the immune system is disrupted in certain conditions, such as autoimmune diseases and infections.[30] Importantly, gonadectomy could be a trigger for autoimmune disorders. In particular, the lack of androgens caused due to castration could lead to autoimmune disorders; this has been reported in a man who underwent testicular removal followed by estrogen administration therapy, and developed SLE.[31] The lack of immunosuppressive function of androgen could result in excessive activation of immune cell proliferation in Yaa as well. However, there was no influence of castration on BXSB immunological condition during the examination period, and there was no treatment-related difference in autoantibody levels in both the BXSB and the Yaa. Thus, male hormones could be important in suppressing autoimmunity, particularly, cellular immunity, but their absence would not affect the immune system if it is functioning normally in this experimental model.

Yaa represents lupus nephritis-like glomerulonephritis with the progression of systemic autoimmune disease. At three months, Yaa showed MPGN, but there was no treatment-related difference in renal pathology except for PEC flattening, suggesting that androgen would not be involved in the onset of Yaa glomerulonephritis, although castration significantly decreased kidney weight. Importantly, female BXSB also developed splenomegaly and MPGN 10 months onwards,[22] while no renal lesion was observed in male BXSB without *Yaa* mutation at the same age. The present study adds evidence that androgens do not directly affect BXSB renal pathologies. These findings indicate that predispositions of the BXSB genome, including the development of MPGN, can be more sensitively affected by estrogen than androgens, even if there is a subsequent effect of androgens.

More severe glomerular pathology characterized by the expansion of sclerotic lesions in the glomerulus in six-month-old Yaa would be associated with autoimmune disease progression, as shown by a positive correlation with spleen weight. On the other hand, castrated Yaa clearly showed milder sclerotic lesions compared with the sham-operated group, whereas there were no treatment differences in nuclear number and glomerular area. These results strongly suggest that formation of sclerotic lesions would be specifically affected by androgens in Yaa, even though

Table 3. Correlation analysis among examined parameters in six-month-old Yaa.

Parameters		Autoimmune disease		Activation of PECs		
		Spleen weight	Serum dsDNA level	CD44-positive PEC number	CD44-positive renal corpuscle ratio	Total PEC number
Sclerotic lesion						
Sclerotic lesion area	ρ	0.515*	0.003	0.863**	0.851**	0.649**
	P	0.029	0.991	<0.001	<0.001	0.004
Sclerotic lesion fraction	ρ	0.302	−0.124	0.655**	0.638**	0.645**
	P	0.223	0.649	0.003	0.004	0.004
Glomerular function						
uACR	ρ	0.612	0.297	0.794**	0.818**	0.527
	P	0.060	0.405	0.006	0.004	0.117
Activation of PECs						
CD44-positive PEC number	ρ	0.417	0.196	–	0.994**	0.723**
	P	0.085	0.468	–	<0.001	0.001
CD44-positive renal corpuscle ratio	ρ	0.475*	0.210	0.994**	–	0.719**
	P	0.047	0.434	<0.001	–	0.001

*$P < 0.05$, **$P < 0.01$. ρ: Spearman's rank correlation coefficient, $n = 18$. uACR: urinary albumin creatinine ratio; PEC: parietal epithelial cell.

androgen was suggested to have a protective effect in other autoimmune nephritis models. Several studies have reported that androgens promote the formation of sclerotic lesions in the glomerulosclerosis disease model. [15] The etiology has not been elucidated, but increase in transforming growth factor-β (TGF-β) level in the glomerulus by androgens could be a potent pathogenesis of glomerular sclerotic lesions. [9] Based on these results, autoimmune nephritis in Yaa would be complicatedly formed by genetic factors, systemic autoimmunity, and sex hormones, but the effect of androgens would be superior to immunosuppression. In addition, salt-sensitive rats exhibited decreased urinary albumin levels and glomerular sclerotic portion following the reduction of blood pressure by castration, [32] suggesting that androgens contribute to systemic and local kidney homeostasis.

Formation of glomerular sclerotic lesions is commonly observed in various kidney diseases, including focal segmental glomerulosclerosis, diabetes nephritis, and lupus nephritis, characterized by ECM accumulations. [33] Disruption of the glomerular filtration barrier that podocytes maintain is the primary pathological event, which results in the leakage of circulating proteins into primitive urine. Previous studies reported that mouse podocytes and mesangial cells express AR, and androgens have been suggested to induce apoptosis of cultured podocytes and promote ECM production in mesangial cells *in vivo*. [7–9] However, in the current model, AR was observed significantly in the nuclei of PECs, but not in those of podocytes and mesangial cells. Importantly, PEC is suggested to be involved in the formation of glomerular sclerotic lesions once podocytes are injured, although the molecular mechanisms are still poorly defined. [24] PECs tend to proliferate, produce ECM, and migrate to tuft to seal the disrupted filtration barrier. As a result, glomeruli increase sclerotic lesions due to the accumulation of ECM that PECs and mesangial cells mainly produce.

Recently, PECs have been divided into subpopulations classified by specific molecules, [26] and CD44 has been established as a marker of activated PECs. [34] CD44 is a cell membrane protein and has been reported to mediate many cellular processes including cell proliferation, migration, and malignancy in various cancers, such as prostate cancer and breast cancer. [35] In addition, CD44 expression reinforces epithelial-mesenchymal transition (EMT) in cancer cells via the TGF-β signaling pathway. [36] ECM components, such as hyaluronic acid and collagen, are ligands for CD44, which signals primarily through the RAS/MAPK or PI3K/Akt pathways. [37] In pathological conditions, CD44-positive PECs are considered to have the ability to proliferate, migrate, and produce ECM as well as cancer cells. Further, previous studies have reported a contribution of CD44-positive PECs to the formation of glomerulosclerosis and crescents. [25] Although the details of CD44-mediated signaling pathway in PECs are unclear, multiple cellular processes, including proliferation, migration, and ECM production would depend on RAS/MAPK or PI3K/Akt signaling during the pathogenesis of glomerular sclerosis, as they do in cancer cells. Our results confirmed CD44 expression on PECs facing injured glomeruli, but not in

renal corpuscles with uninjured glomeruli, and a positive correlation with sclerotic indices indicated CD44 function in the formation of sclerotic lesions in Yaa. Additionally, the decreased number of CD44-positive PECs and the positive ratio of CD44 in the renal corpuscles of six-month-old castrated Yaa highlighted the effect of androgens on CD44 expression. The decreased number of Ki67-positive PECs suggests that the proliferation of PEC is suppressed in castrated Yaa, which might result in the decrease of total number of PECs. Thus, we infer that morpho-functional changes in PECs under androgen-poor conditions play a key role in the attenuation of glomerular sclerosis in Yaa.

AR is stably expressed in the cytoplasm of widespread cells and tissues. After androgens bind to AR, androgen/AR (A/AR) complexes translocate to the nucleus and function as transcription factors by binding to AREs specifically. [28,38] Importantly, the involvement of A/AR signaling in CD44 expression has been suggested in some epithelial tumors. Prostate cancer develops androgen-dependently, and *in vitro* analysis showed that AR expression mediates CD44 expression in prostate cancer cells. [39,40] In this study, we discovered that half site motifs of ARE are present in the promoter region of *Cd44*, even though the full sequence, 5′-AGAACANNNTGTTCT-3′ was not found. These results suggest that androgens regulate *Cd44* expression in cooperation with other transcription factors. Furthermore, androgen-mediated CD44 expression is related to EMT in cancer cells, which allows cells to proliferate and produce ECM excessively. [41] In renal pathology, PECs expressing CD44 are observed to undergo the EMT, resulting in the proliferation and production of ECM, thereby forming crescent and glomerular sclerotic lesions. [42] Thus, we conclude that A/AR might mediate the PEC phenotype by regulating CD44 expression in Yaa glomerulonephritis. Moreover, decreased immunopositive reaction of AR in the PEC nucleus in castrated mice compared with sham-operated PEC, despite equivalent mRNA expression levels of *Ar* in the whole kidney, supported the decreased activity of A/AR signaling pathway, owing to castration.

Castrated Yaa showed decreased levels of uACR compared to the sham group at four months, when MPGN progressed severely in Yaa. This suggests that castration prevents progression of renal lesions in Yaa. There is a less possibility of direct contribution of androgens to glomerular injury because there is no expression of AR in the glomerulus. It is rather reasonable that androgens had already affected PECs at four months to promote the formation of sclerotic lesions. Androgen is thought to increase albuminuria in some strains of mice and rats, as male animals show higher urinary protein levels than females. [43,44] The pathogenesis is still unclear, but androgen-dependent hypertension could lead to leakage of albumin into urine. [31] Importantly, albuminuria from glomeruli has been reported to induce CD44 expression in PECs in a glomerulonephritis mouse model via RAS/MAPK signaling. [45] Positive correlation between CD44-related indices and uACR level in six-month-old Yaa indicates their close association with Yaa as well. Higher uACR levels in sham-operated Yaa than in the castrated group at four and

....

five months suggest that androgens induce the leakage of albumin, which could enhance CD44 expression in PECs. As a result, formation of glomerular sclerosis lesions synergistically exacerbated renal pathology in Yaa. However, at the late disease stage, castrated Yaa showed equivalent levels of uACR with sham-operated Yaa. It could be reasoned that castrated Yaa developed more severe autoimmune diseases and MPGN than in early stages, and the formation of global sclerotic lesions in sham-operated Yaa leads to glomerular dysfunction, resulting in decreased uACR level.

In conclusion, castration caused accelerated onset of autoimmune disease, but attenuated sclerotic lesions in Yaa, a male-dominant autoimmune disease mouse model. In the pathogenesis of autoimmune disease, androgen suppresses excessive autoimmune reactions expressed earlier during the onset of disease in castrated Yaa. In contrast, renal pathology is definitely exacerbated with the expansion of sclerotic lesions in the presence of androgen. Our results suggest the importance of the effect of androgen on the formation of glomerular sclerosis over the immunosuppressive effect in this autoimmune glomerulonephritis model. In particular, A/AR signaling mediates PEC phenotypes to proliferate and produce ECM in disease conditions by activating CD44 expression, which could result in the formation of glomerular sclerosis lesions in Yaa. These findings provide novel insights into the sex-related disparity of renal diseases in zoobiquitous medicine.

AUTHORS' CONTRIBUTIONS

YO, OI, TN, and YK designed the work; YO, OI, MA, and TN performed experiments and analyzed the data; YO, OI, and YK drafted and revised the manuscript. All the authors were involved in the writing of the paper and approval of the final manuscript.

DECLARATION OF CONFLICTING INTERESTS

The author(s) declared no potential conflicts of interest with respect to the research, authorship, and/or publication of this article.

ORCID iDs

Md. Abdul Masum https://orcid.org/0000-0003-3049-3777
Teppei Nakamura https://orcid.org/0000-0003-3204-0245
Yasuhiro Kon https://orcid.org/0000-0003-0224-6197

SUPPLEMENTAL MATERIAL

Supplemental material for this article is available online.

REFERENCES

1. Ortona E, Pierdominici M, Maselli A, Veroni C, Aloisi F, Shoenfeld Y. Monographic section sex-based differences in autoimmune diseases. *Ann Ist Super Sanità* 2016;**52**:205–12
2. Yung S, Chan TM. Mechanisms of kidney injury in lupus nephritis - the role of anti-dsDNA antibodies. *Front Immunol* 2015;**6**:475
3. Hsu CY, Chiu WC, Yang TS, Chen CJ, Chen YC, Lai HM, Yu SF, Su YJ, Cheng TT. Age- and gender-related long-term renal outcome in patients with lupus nephritis. *Lupus* 2011;**20**:1135–41
4. Schwartzman-Morris J, Putterman C. Gender differences in the pathogenesis and outcome of lupus and of lupus nephritis. *Clin Dev Immunol* 2012;**2012**:604892
5. Li Q, McDonough AA, Layton H, Layton A. Functional implications of sexual dimorphism of transporter patterns along the rat proximal tubule: modeling and analysis. *Am J Physiol Ren Physiol* 2018;**315**:692–700
6. Bardin CW, Catterall JF. Testosterone: a major determinant of extragenital sexual dimorphism. *Science* 1981;**211**:1285–94
7. Sabolić I, Asif AR, Budach WE, Wanke C, Bahn A, Burckhardt G. Gender differences in kidney function. *Pflugers Arch* 2007;**455**:397–429
8. Doublier S, Lupia E, Catanuto P, Periera-Simon S, Xia X, Korach K, Berho M, Elliot SJ, Karl M. Testosterone and 17B-estradiol have opposite effects on podocyte apoptosis that precedes glomerulosclerosis in female estrogen receptor knockout mice. *Kidney Int* 2011;**79**:404–13
9. Elliot SJ, Berho M, Korach K, Doublier S, Lupia E, Striker GE, Karl M. Gender-specific effects of endogenous testosterone: female α-estrogen receptor-deficient C57Bl/6J mice develop glomerulosclerosis. *Kidney Int* 2007;**72**:464–72
10. Neugarten J, Golestaneh L. Influence of sex on the progression of chronic kidney disease. *Mayo Clin Proc* 2019;**94**:1339–59
11. Silbiger SR, Neugarten J. The impact of gender on the progression of chronic renal disease. *Am J Kidney Dis* 1995;**25**:515–33
12. Carrero JJ. Gender differences in chronic kidney disease: underpinnings and therapeutic implications. *Kidney Blood Press Res* 2010;**33**:383–92
13. Cho MH, Jung K-J, Jang H-S, Kim JI, Park KM. Orchiectomy attenuates kidney fibrosis after ureteral obstruction by reduction of oxidative stress in mice. *Am J Nephrol* 2012;**35**:7–16
14. Soljancic A, Ruiz AL, Chandrashekar K, Maranon R, Liu R, Reckelhoff JF, Juncos LA. Protective role of testosterone in ischemia-reperfusion-induced acute kidney injury. *Am J Physiol Integr Comp Physiol* 2013;**304**:951–8
15. Inada A, Inada O, Fujii NL, Nagafuchi S, Katsuta H, Yasunami Y, Matsubara T, Arai H, Fukatsu A, Nabeshima YI. Adjusting the 17β-estradiol-to-androgen ratio ameliorates diabetic nephropathy. *J Am Soc Nephrol* 2016;**27**:3035–50
16. Kattah AG, Smith CY, Rocca LG, Grossardt BR, Garovic VD, Rocca WA. CKD in patients with bilateral oophorectomy. *Clin Am J Soc Nephrol* 2018;**13**:1649–58
17. Ichii O, Konno A, Sasaki N, Endoh D, Hashimoto Y, Kon Y. Onset of autoimmune glomerulonephritis derived from the telomeric region of MRL-chromosome 1 is associated with the male sex hormone in mice. *Lupus* 2009;**18**:491–500
18. Roubinian JR, Talal N, Greenspan JS, Goodman JR, Siiteri PK. Effect of castration and sex hormone treatment on survival, anti-nucleic acid antibodies, and glomerulonephritis in NZB/NZW F1 mice. *J Exp Med* 1978;**147**:1568–83
19. Suzuka H, Yoshifusa H, Nakamura Y, Miyawaki S, Shibata Y. Morphological analysis of autoimmune disease in MRL-lpr, Yaa male mice with rapidly progressive systemic lupus erythematosus. *Autoimmunity* 1993;**14**:275–82
20. Kimura J, Ichii O, Otsuka S, Sasaki H, Hashimoto Y, Kon Y. Close relations between podocyte injuries and membranous proliferative glomerulonephritis in autoimmune murine models. *Am J Nephrol* 2013;**38**:27–38
21. Murphy ED, Roths JB. A y chromosome associated factor in strain bxsb producing accelerated autoimmunity and lymphoproliferation. *Arthritis Rheum* 1979;**22**:1188–94

22. Kimura J, Ichii O, Nakamura T, Horino T, Otsuka S, Kon Y. BXSB-type genome causes murine autoimmune glomerulonephritis: pathological correlation between telomeric region of chromosome 1 and yaa. *Genes Immun* 2014;**15**:182–9

23. Eisenberg RaDixon FJ. Effect of castration on male-determined acceleration of autoimmune disease in BXSB mice. *J Immunol* 1980;**125**:1959–61

24. Nagata M. Podocyte injury and its consequences. *Kidney Int* 2016;**89**:1221–30

25. Eymael J, Sharma S, Loeven MA, Wetzels JF, Mooren F, Florquin S, Deegens JK, Willemsen BK, Sharma V, van Kuppevelt TH, Bakker MA, Ostendorf T, Moeller MJ, Dijkman HB, Smeets B, van der vlag J. CD44 is required for the pathogenesis of experimental crescentic glomerulonephritis and collapsing focal segmental glomerulosclerosis. *Kidney Int* 2018;**93**:626–42

26. Kuppe C, Leuchtle K, Wagner A, Kabgani N, Saritas T, Puelles VG, Smeets B, Hakroush S, van der Vlag J, Boor P, Schiffer M, Gröne HJ, Fogo A, Floege J, Moeller MJ. Novel parietal epithelial cell subpopulations contribute to focal segmental glomerulosclerosis and glomerular tip lesions. *Kidney Int* 2019;**96**:80–93

27. Roche PJ, Hoare SA, Parker MG. A consensus DNA-binding site for the androgen receptor. *Mol Endocrinol* 1992;**6**:2229–35

28. Wilson S, Qi J, Filipp FV. Refinement of the androgen response element based on ChIP-Seq in androgen-insensitive and androgen-responsive prostate cancer cell lines. *Sci Rep* 2016;**6**:15

29. Vanderschueren D, Vandenput L, Boonen S, Lindberg MK, Bouillon R, Ohlsson C. Androgens and bone. *Endocr Rev* 2004;**25**:389–425

30. Lin TF. *The 5-minute pediatric consult. 8th ed. [Wolters Kluwer health].* Philadelphia, PA: Lippincott Williams & Wilkins, 2018, pp.870–1

31. Pontes LT, Camilo DT, De Bortoli MR, Santos RSS, Luchi WM. New-onset lupus nephritis after male-to-female sex reassignment surgery. *Lupus* 2018;**27**:2166–9

32. Yanes LL, Sartori-Valinotti JC, Iliescu R, Romero DG, Racusen LC, Zhang H, Reckelhoff JF. Testosterone-dependent hypertension and upregulation of intrarenal angiotensinogen in dahl salt-sensitive rats. *Am J Physiol Renal Physiol* 2009;**296**:F771–9

33. Djudjaj S, Boor P. Cellular and molecular mechanisms of kidney fibrosis. *Mol Aspects Med* 2019;**65**:16–36

34. Fatima H, Moeller MJ, Smeets B, Yang HC, VD, Alpers CE, Fogo AB. Parietal epithelial cell activation marker in early recurrence of FSGS in the transplant. *Clin J Am Soc Nephrol* 2012;**7**:1852–8

35. Senbanjo LT, Chellaiah MA. CD44: a multifunctional cell surface adhesion receptor is a regulator of progression and metastasis of cancer cells. *Front Cell Dev Biol* 2017;**5**:18

36. Takahashi E, Nagano O, Ishimoto T, Yae T, Suzuki Y, Shinoda T, Nakamura S, Niwa S, Ikeda S, Koga H, Tanihara H, Saya H. Tumor necrosis factor-α regulates transforming growth factor-β-dependent epithelial-mesenchymal transition by promoting hyaluronan-CD44-moesin interaction. *J Biol Chem* 2010;**285**:4060–73

37. Chen C, Zhao S, Karnad A, Freeman JW. The biology and role of CD44 in cancer progression: therapeutic implications. *J Hematol Oncol* 2018;**11**:64

38. Davey RA, Grossmann M. Androgen receptor structure, function and biology: from bench to bedside. *Clin Biochem Rev* 2016;**37**:3–15

39. Srinivasan D, Senbanjo L, Majumdar S, Franklin RB, Chellaiah MA. Androgen receptor expression reduces stemness characteristics of prostate cancer cells (PC3) by repression of CD44 and SOX2. *J Cell Biochem* 2019;**120**:2413–28

40. Ghatak S, Hascall VC, Markwald RR, Misra S. Stromal hyaluronan interaction with epithelial CD44 variants promotes prostate cancer invasiveness by augmenting expression and function of hepatocyte growth factor and androgen receptor. *J Biol Chem* 2010;**285**:19821–32

41. Matuszak EA, Kyprianou N. Androgen regulation of epithelial-mesenchymal transition in prostate tumorigenesis. *Expert Rev Endocrinol Metab* 2011;**6**:469–82

42. GS, Chandra V, Phadnis S, Bhonde R. Glomerular parietal epithelial cells of adult murine kidney undergo EMT to generate cells with traits of renal progenitors. *J Cell Mol Med* 2011;**15**:396–413

43. Long DA, Kolatsi-Joannou M, Price KL, Dessapt-Baradez C, Huang JL, Papakrivopoulou E, Hubank M, Korstanje R, Gnudi L, Woolf AS. Albuminuria is associated with too few glomeruli and too much testosterone. *Kidney Int* 2013;**83**:1118–29

44. Remuzzi A, Puntorieri S, Mazzoleni A, Remuzzi G. Sex related differences in glomerular ultrafiltration and proteinuria in Munich-Wistar rats. *Kidney Int* 1988;**34**:481–6

45. Zhao X, Chen X, Chima A, Zhang Y, George J, Cobbs A, Emmett N. Albumin induces CD44 expression in glomerular parietal epithelial cells by activating extracellular signal-regulated kinase 1/2 pathway. *J Cell Physiol* 2019;**234**:7224–35